J. DIFERENSIAL/E-ISSN:2775-9644
Vol.8(2),2026, 201–218
doi:https://doi.org/10.35508/jd.v8i2.30625

RESEARCH ARTICLE

Fuzzy TOPSIS Ranking Stability under Membership-Function Variations across Alternative-Closeness Scenarios

Mohammad Nafie Jauhari[1*], Muhammad Khudzaifah[1], Ria Dhea Layla Nur Karisma[1], Juhari[1], Heni Widayani[1], Dewi Ismiarti[1], Intan Nisfulaila[1]

[1]*Department of Mathematics, Faculty of Science and Technology, Universitas Islam Negeri Maulana Malik Ibrahim Malang, Indonesia*
[*]*Corresponding author: nafie.jauhari@uin-malang.ac.id*

Received: 8 October 2026; Revised: 18 October 2026; Accepted: 30 October 2026; Published: 7 November 2026.

Abstract: This study examines how alternative closeness and membership-function geometry jointly affect ranking stability in a membership-function-based Fuzzy TOPSIS variant. The Energy Efficiency Dataset was normalized into three criteria, and sliding windows of 20 alternatives were selected to represent strong dominance, moderate competition, and tight competition. Triangular, trapezoidal, and Gaussian membership functions were compared under identical linguistic centres and equal criterion weights. Membership degrees were aggregated into crisp criterion scores before the standard TOPSIS distance procedure was applied. Stability was evaluated using rank displacement, Spearman's correlation, and tie-adjusted Kendall's tau-b. Under strong dominance, the mean rank displacement was 1.45 positions and all pairwise correlations were high. Moderate competition produced the largest mean displacement (4.20 positions), whereas tight competition produced a maximum shift of 10 positions. In the tightest scenario, triangular and Gaussian rankings remained nearly identical (Spearman's $\rho = 0.9985$; Kendall's $\tau_b = 0.9894$), while pairs involving the trapezoidal function declined to $\tau_b \approx 0.56$. The plateau of the trapezoidal function reduced discrimination among adjacent values and amplified rank changes. These results show that ranking stability depends on the interaction between data structure and membership-function shape. Alternative-closeness diagnostics and cross-function stability checks should therefore accompany applications of this Fuzzy TOPSIS variant involving closely matched alternatives.

Keywords: Fuzzy TOPSIS; membership functions; ranking stability; rank reversal; alternative closeness

1. Introduction

Multi-criteria decision-making (MCDM) provides a framework for evaluating alternatives when criteria differ in scale, preference direction, and relative importance. Within this framework, decision outcomes are determined not only by the original data but also by a sequence of methodological choices involving normalization, weighting, aggregation, and ranking [1–3]. The *Technique for Order Preference by Similarity to Ideal Solution* (TOPSIS) remains widely developed because it relies on an intuitively interpretable geometric principle: a selected alternative should be close to the positive ideal

© Jauhari *et al.*

solution and distant from the negative ideal solution [4, 5]. This simplicity does not automatically guarantee robust rankings, because changes in data transformation or model configuration may alter interpoint distances, closeness coefficients, and the ordering of alternatives.

Recent methodological studies increasingly regard normalization and weighting as substantive decisions rather than neutral preprocessing stages. Comparisons of normalization techniques show that different formulas can produce different preference values and rankings even when the decision matrix remains unchanged [6, 7]. Along the same line, combinations of normalization and weighting schemes have been assessed using correlation and ranking-dissimilarity measures to evaluate TOPSIS robustness [8, 9]. More recent studies further indicate that data-distribution structure, weighting methods, and the treatment of cost criteria may affect ranking stability [10, 11]. These findings demonstrate that an MCDM ranking is an outcome of the interaction between data and modelling assumptions rather than a purely mechanical consequence of the data.

When assessments are linguistic, ambiguous, or not precisely expressible, Fuzzy TOPSIS extends TOPSIS by representing criterion values and preferences through fuzzy sets or fuzzy numbers. Early formulations of Fuzzy TOPSIS provided a mechanism for processing group assessments in a fuzzy environment [12], whereas subsequent studies developed Fuzzy AHP–TOPSIS integrations and diverse uncertainty representations [13]. Recent developments have moved towards richer representations, including *continuous intuitionistic fuzzy sets*, type-2 fuzzy numbers, circular fuzzy information, and interval-valued analysis [14–17]. These developments primarily aim to preserve linguistic information, accommodate more complex uncertainty, or improve ranking indices. However, richer representations also entail a greater number of modelling choices before a ranking is obtained.

One fundamental choice is the shape of the membership function. Triangular, trapezoidal, and Gaussian functions employ different geometries to map a value to a degree of membership: triangular functions have a single peak, trapezoidal functions have a flat core region, and Gaussian functions provide smooth transitions without sharply bounded support. Structured reviews of membership functions indicate that no single form is superior for all data types and systems; their effectiveness depends on problem characteristics, parameter construction, and modelling objectives [18, 19]. Recent literature has consequently moved towards data-driven membership-function construction, parameter optimization, linguistic-term semantics, and expert elicitation [20–22]. Membership-function shape is therefore not merely a visual choice. It determines which regions of the domain are preserved, compressed, or treated as equivalent before information enters the TOPSIS procedure.

Several studies have shown that the representation of fuzzy data can directly affect TOPSIS outcomes. Comparisons of TOPSIS under crisp and fuzzy inputs have reported classification differences when fuzzy data are operated on directly or are first converted into crisp values using particular membership functions [23]. Other studies have proposed new ranking indices to reduce misleading priorities [24], retained interval-valued outputs in type-2 Fuzzy TOPSIS [15], or delayed defuzzification to prevent the premature loss of linguistic information [17]. These findings reinforce the view that fuzzy-representation and transformation stages can alter the discriminative capacity of the model. Nevertheless, their principal focus lies in developing new representations or indices rather than in conducting a controlled test of the consequences of three membership-function geometries under the same data and TOPSIS procedure.

In this study, the term *Fuzzy TOPSIS* denotes a membership-function-based variant rather than a formulation that retains fuzzy numbers throughout all TOPSIS operations. Normalized criterion values are evaluated through fuzzy membership functions and then converted into single operational scores by a membership-weighted average of linguistic centres. The subsequent ideal-solution, distance, and closeness-coefficient calculations use standard crisp TOPSIS. This deliberate design isolates the effect of membership-function geometry at the transformation stage; it should therefore be distinguished from conventional Fuzzy TOPSIS approaches that perform distance calculations directly on fuzzy numbers.

In parallel, the ranking-stability literature examines *rank reversal*, namely changes in the relative ordering of alternatives when the alternative set, normalization technique, weights, or method configuration changes. This phenomenon has been analysed in TOPSIS through critical studies, improvements to ideal points, and methods designed to preserve ranking order [25, 26]. Larger-scale simulation experiments indicate that the likelihood of *rank reversal*, tie formation, and tie breaking is affected by the MCDM method and the design of changes to alternatives [27]. TOPSIS sensitivity studies have also focused extensively on normalization, weights, or comparisons between methods [8, 9, 11]. Within this body of work, membership-function geometry has not been sufficiently positioned as a sensitivity factor to be examined jointly with the closeness structure of alternatives.

Closeness among alternatives is important because an identical score perturbation need not have identical ordinal consequences. When performance differences are relatively wide, small deviations in fuzzy scores may be absorbed without changing the order. Conversely, for nearly equivalent alternatives, small changes induced by membership transformation may exceed score margins and shift several positions simultaneously. Stability should therefore be assessed not only through score similarity but also through the number of alternatives that move, the magnitude of positional shifts, and overall ranking agreement measured by Spearman's correlation and Kendall's tau-b [27–29]. This perspective links the geometry of fuzzy transformation to the competitive structure embedded in the data.

The central issue is thus not the absence of research on Fuzzy TOPSIS, membership functions, or *rank reversal*, but the lack of a consolidated relationship between membership-function geometry, alternative closeness, and ranking stability within a comparable experimental framework. This study compares triangular, trapezoidal, and Gaussian functions across three scenarios representing strong dominance, moderate competition, and tight competition. All scenarios employ controlled transformation and TOPSIS procedures, weights, and baseline parameters so that ranking changes can be traced to membership-function shape and alternative structure. Stability is evaluated through positional shifts, the number of changed alternatives, Spearman's correlation, and Kendall's tau-b. The contribution of this study lies in explaining a conditional mechanism: geometric differences become more consequential as alternative margins narrow, particularly when the flat region of a trapezoidal function reduces discriminative information before distances to the ideal solutions are computed.

2. Methods

2.1. Data and Preprocessing

The experiment used the *Energy Efficiency Dataset* from the UCI Machine Learning Repository [30]. The dataset contains 768 building configurations, each of which was treated as a decision alternative. Three variables were used as criteria: *relative compactness* as a *benefit* criterion, and *heating load* and *cooling load* as *cost* criteria. This selection produced a decision matrix of dimension 768×3.

Each criterion was normalized to $[0, 1]$ so that all criteria had the same preference direction. For alternative i and criterion j, normalization was defined as

$$r_{ij} = \begin{cases} \dfrac{x_{ij} - \min_i x_{ij}}{\max_i x_{ij} - \min_i x_{ij}}, & \text{benefit criterion,} \\ \dfrac{\max_i x_{ij} - x_{ij}}{\max_i x_{ij} - \min_i x_{ij}}, & \text{cost criterion.} \end{cases} \tag{2.1}$$

After normalization, a larger value consistently indicated better performance.

2.2. Construction of Alternative-Closeness Scenarios

Scenarios were constructed before the membership-function transformation and TOPSIS procedure were applied to avoid circular bias. Initial aggregate scores were calculated using equal weights,

$w_1 = w_2 = w_3 = 1/3$, as follows:

$$s_i = \sum_{j=1}^{3} w_j r_{ij}. \tag{2.2}$$

Equal weights were used as an experimental control rather than as a claim that the three criteria are universally equally important. Fixing the weights prevents an elicited or data-driven weighting scheme from becoming an additional source of variation, so differences across the experimental runs can be attributed more directly to membership-function geometry and alternative closeness. Weight sensitivity remains outside the scope of the present experiment.

Alternatives were ordered by s_i, after which consecutive windows W_t of size $k = 20$ were formed. The degree of closeness was measured by the range

$$R(W_t) = \max_{A_i \in W_t} s_i - \min_{A_i \in W_t} s_i. \tag{2.3}$$

For a fixed-size window ordered by s_i, $R(W_t)$ is the maximum pairwise separation between aggregate scores. A small range confines every alternative in the window to a narrow score interval and therefore represents closer competition; a large range indicates stronger separation within the same number of alternatives. The range is transparent and scale-interpretable, although it summarizes only the endpoints rather than the complete within-window distribution. The window with the largest $R(W_t)$ was used as the strong-dominance scenario (S1), the window closest to the median of the $R(W_t)$ distribution as the moderate-competition scenario (S2), and the window with the smallest range as the tight-competition scenario (S3). These names are operational labels for the selected points in this dataset, not universal thresholds. In the event of equal range values, the window with the smallest starting index was selected to ensure a deterministic procedure.

2.3. Membership-Function Transformation

The normalized values r_{ij} were evaluated against five linguistic labels with centres

$$c_l \in \{0, 0.25, 0.50, 0.75, 1.00\}.$$

The three membership functions compared were triangular (T), trapezoidal (Z), and Gaussian (G):

$$\mu_l^T(r) = \max\left(0, 1 - \frac{|r - c_l|}{h}\right), \tag{2.4}$$

$$\mu_l^Z(r) = \begin{cases} 0, & |r - c_l| \geq b, \\ \dfrac{b - |r - c_l|}{b - a}, & a < |r - c_l| < b, \\ 1, & |r - c_l| \leq a, \end{cases} \tag{2.5}$$

$$\mu_l^G(r) = \exp\left[-\frac{(r - c_l)^2}{2\sigma^2}\right]. \tag{2.6}$$

The fundamental geometries of the three functions are shown in Figure 2.1. The triangular function has a single peak and linear slopes, the trapezoidal function has a plateau that provides a full-membership interval, and the Gaussian function changes smoothly with asymptotic tails. These differences provide the basis for the transformation responses examined in the experiment.

The parameters were set consistently with the distance between adjacent centres: $h = 0.25$, $a = 0.125$, $b = 0.25$, and $\sigma = 0.125$. With identical centres, the resulting differences primarily reflected curve geometry. The membership degrees were aggregated into a single crisp transformed score using the membership-weighted average of label centres,

$$q_{ij}^F = \frac{\sum_{l=1}^{5} \mu_l^F(r_{ij}) c_l}{\sum_{l=1}^{5} \mu_l^F(r_{ij})}, \qquad F \in \{T, Z, G\}. \tag{2.7}$$

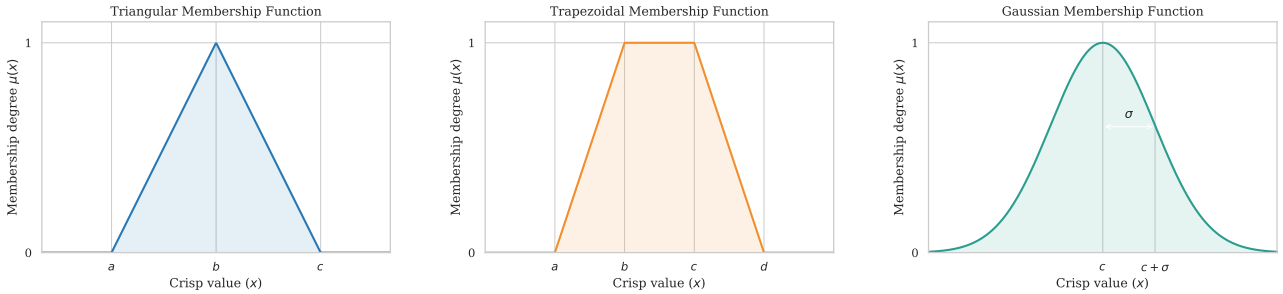


Figure 2.1: Fundamental Geometries of the Triangular, Trapezoidal, and Gaussian Membership Functions

2.4. Membership-Function-Based TOPSIS and Stability Assessment

Equation (2.7) completes the fuzzy transformation stage: q_{ij}^F is crisp rather than a fuzzy number. Thus, for each scenario–membership-function combination, the remaining calculations follow standard crisp TOPSIS. The weighted matrix was calculated as $v_{ij}^F = w_j q_{ij}^F$. Because all criteria had been oriented as *benefit* criteria, the positive and negative ideal solutions were $A_j^+ = \max_i v_{ij}^F$ and $A_j^- = \min_i v_{ij}^F$, respectively. Euclidean distances and closeness coefficients were calculated as

$$D_i^+ = \sqrt{\sum_{j=1}^{3}(v_{ij}^F - A_j^+)^2}, \qquad D_i^- = \sqrt{\sum_{j=1}^{3}(v_{ij}^F - A_j^-)^2}, \tag{2.8}$$

$$CC_i = \frac{D_i^-}{D_i^+ + D_i^-}. \tag{2.9}$$

Alternatives were ranked in descending order of CC_i.

Stability was compared for three ranking pairs: $T - Z$, $T - G$, and $Z - G$. In addition to the number of alternatives that changed position and the mean and maximum positional shifts, Spearman's correlation and tie-adjusted Kendall's tau-b were used. For two rank vectors R and S, these coefficients were computed as

$$\rho = \mathrm{corr}(R, S), \qquad \tau_b = \frac{C - D}{\sqrt{(C + D + T_R)(C + D + T_S)}}, \tag{2.10}$$

where C and D denote concordant and discordant pairs, while T_R and T_S count pairs tied only in R and only in S, respectively. Ranks were assigned in descending order of CC_i; tied values received their average rank. No ties occurred in S1 or S2. In S3, A188 and A284 were tied under all three membership functions and therefore received average ranks. Spearman's coefficient was calculated from these average-rank vectors, and Kendall's tau-b explicitly corrected for ties. Values close to one indicate stronger ranking agreement. All stages were implemented in Python using `pandas`, `numpy`, and `scipy.stats`.

3. Results and Discussion

3.1. Data Validation and Alternative-Closeness Scenarios

The experiment involved 768 alternatives without missing values. Before normalization, *relative compactness* ranged from 0.62 to 0.98, whereas *heating load* and *cooling load* ranged from 6.01 to 43.10 and from 10.90 to 48.03, respectively. These scale differences disappeared after min–max normalization, although the distributional shapes remained distinct: the means of the normalized values for

the three criteria were 0.4005, 0.5606, and 0.6314, respectively, with standard deviations of 0.2938, 0.2720, and 0.2562. Thus, normalization aligned the ranges without removing heterogeneity in the distributions across criteria.

The initial aggregate scores of all alternatives ranged from 0.1680 to 0.8206, with a mean of 0.5308, a median of 0.5548, and a standard deviation of 0.1362. Among 749 consecutive windows of size 20, the distribution of $R(W_t)$ had a minimum of 0.0020, a median of 0.0092, and a maximum of 0.1051. S1, S2, and S3 were selected precisely at these three diagnostic points (Table 3.1), rather than on the basis of Fuzzy TOPSIS results. This separation is important because it prevents circular bias: the variable to be evaluated was not used to construct the test groups.

Table 3.1: Validation of Alternative-Closeness Scenarios

Scenario	Characteristic	Index	$\bar{s}$	$R(W_t)$	Distribution position
S1	Strong dominance	746–765	0.7390	0.1051	Maximum
S2	Moderate competition	257–276	0.5105	0.0092	Median
S3	Tight competition	307–326	0.5254	0.0020	Minimum

The S1 range was more than ten times the S2 range and more than fifty times the S3 range. Figure 3.1 shows that S2 represents the middle of the window distribution, whereas S1 and S3 capture the two extreme conditions. Changes in stability across scenarios can therefore be interpreted against a controlled competition structure, although these three scenarios are insufficient to establish a continuous population-level relationship.

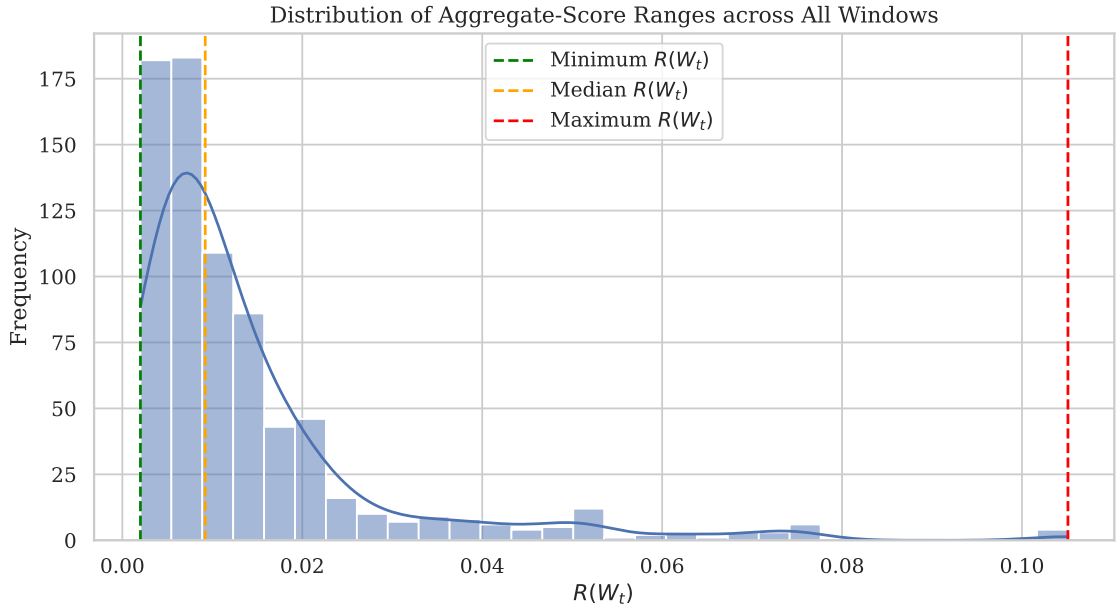


Figure 3.1: Distribution of $R(W_t)$ and the Positions of the Three Experimental Scenarios

The direct comparison in Figure 3.2 clarifies the scale of the differences. The S1 bar is substantially higher than that of S2, whereas the S3 bar lies close to the horizontal axis. This visualization complements the global distribution by displaying the actual range used in each scenario.

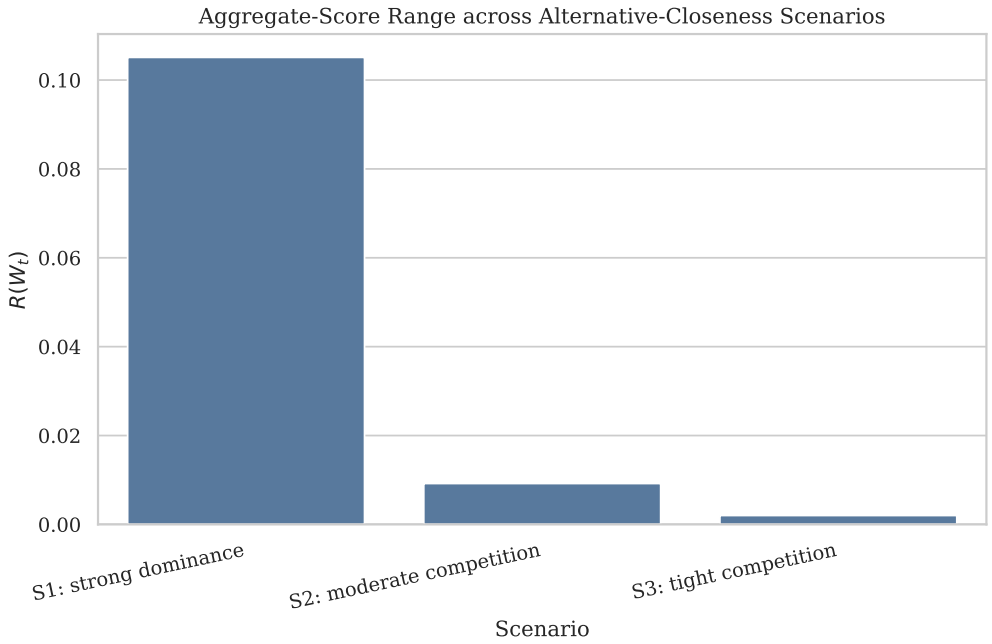


Figure 3.2: Comparison of $R(W_t)$ Values across the Three Experimental Scenarios

3.2. Traces of Membership-Function Transformation

Table 3.2 shows that the three functions produce not only different curve shapes but also different statistical traces in the matrix entering TOPSIS. With equally spaced label centres and $h = 0.25$, the triangular function returned statistics identical to those of the normalized matrix. Under this configuration, $q_{ij}^{T} = r_{ij}$; the triangular function therefore acted as an identity mapping. This conclusion is specific to the experimental parameters and does not imply that every triangular function is necessarily an identity mapping.

Table 3.2: Descriptive Statistics of Transformed Fuzzy Scores q_{ij}

Criterion	Function	Minimum	Maximum	Mean	SD
Relative Compactness	Triangular	0.00000	1.00000	0.40046	0.29383
	Trapezoidal	0.00000	1.00000	0.40224	0.29373
	Gaussian	0.02994	0.97006	0.40147	0.28405
Heating Load	Triangular	0.00000	1.00000	0.56060	0.27205
	Trapezoidal	0.00000	1.00000	0.56425	0.27382
	Gaussian	0.02994	0.97006	0.55964	0.26849
Cooling Load	Triangular	0.00000	1.00000	0.63136	0.25622
	Trapezoidal	0.00000	1.00000	0.63139	0.25418
	Gaussian	0.02994	0.97006	0.62939	0.25360

The trapezoidal function retained the $[0, 1]$ range but shifted the mean and dispersion because its plateau pulled values around label centres towards the same categorical output. The Gaussian function displayed a different pattern: all criteria contracted to approximately $[0.02994, 0.97006]$, and their standard deviations were smaller than those under the triangular function. This contraction is consistent with Gaussian tails, which allow other labels to make small contributions to the aggregate value even near the two ends of the domain.

The five-label linguistic configurations used in the computation are presented in Figure 3.3. Unlike the single-function geometry illustration in the Methods section, this figure shows overlap among the five labels on the normalized domain. The triangular function preserves linear gradients between centres, the trapezoidal function forms several plateau intervals, and the Gaussian function provides smooth cross-label contributions.

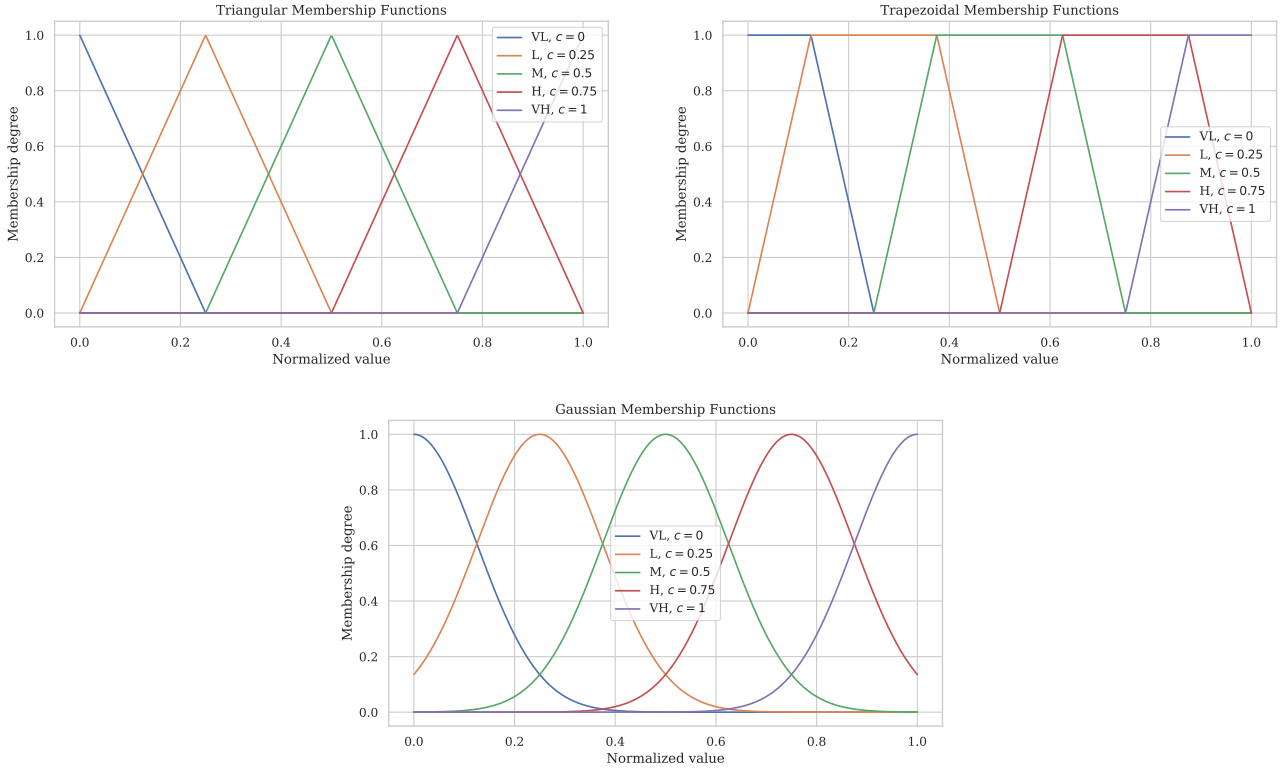


Figure 3.3: Five Linguistic Labels under the Triangular (upper left), Trapezoidal (upper right), and Gaussian (bottom) Functions

The aggregate differences originated from micro-level deviations whose directions were not uniform. For A001, the *relative compactness* value $r_1 = 1.000$ remained 1.000 under the triangular and trapezoidal functions but became 0.970 under the Gaussian function. Conversely, for A005 with $r_1 = 0.778$, the trapezoidal function increased the score to 0.795, whereas the Gaussian function reduced it to 0.774. For other criteria, the trapezoidal function could either increase or decrease a score, depending on the location of the value relative to label centres and plateaus. Because TOPSIS constructs ideal solutions from the entire matrix, these deviations do not operate independently on individual alternatives; they alter the ideal points and the distances of all alternatives simultaneously.

These findings are consistent with the literature, which indicates that membership-function shape has no universal advantage and should be selected according to the data and modelling objective [18, 19]. In the TOPSIS context, the results further specify evidence that transforming fuzzy inputs into operational values can yield different classifications [23]. The present experiment differs in that it holds the TOPSIS procedure and weights constant, allowing the transformation trace to be directly related to the compared geometries.

3.3. Ranking Changes within Each Scenario

3.3.1. S1: Strong Dominance Preserves the Leading Positions

Under S1, the leading alternative did not change when the membership function was replaced. A002 remained in first position, followed by A027, A025, A028, and A026 in the same subsequent five positions. The CC_i values nevertheless shifted; for example, A027 changed from 0.3777 under the triangular function to 0.4009 under the trapezoidal function and 0.3583 under the Gaussian function. However, A002 had CC_i values of approximately 0.675–0.697, so its separation from the following group was sufficiently large to preserve first position.

The stability of S1 was not absolute. Eleven of the 20 alternatives retained their positions, whereas the other nine changed, primarily in the lower part of the ranking. A035 was the most sensitive case: its position changed from 12 under the triangular function to 19 under the trapezoidal function and remained 19 under the Gaussian function. Hence, a wide competitive range protected the macro-order and leading candidates but did not eliminate local exchanges among alternatives that remained close to one another.

Figure 3.4 confirms that lines in the leading positions remained horizontal, whereas crossings were concentrated in the lower part of the ranking.

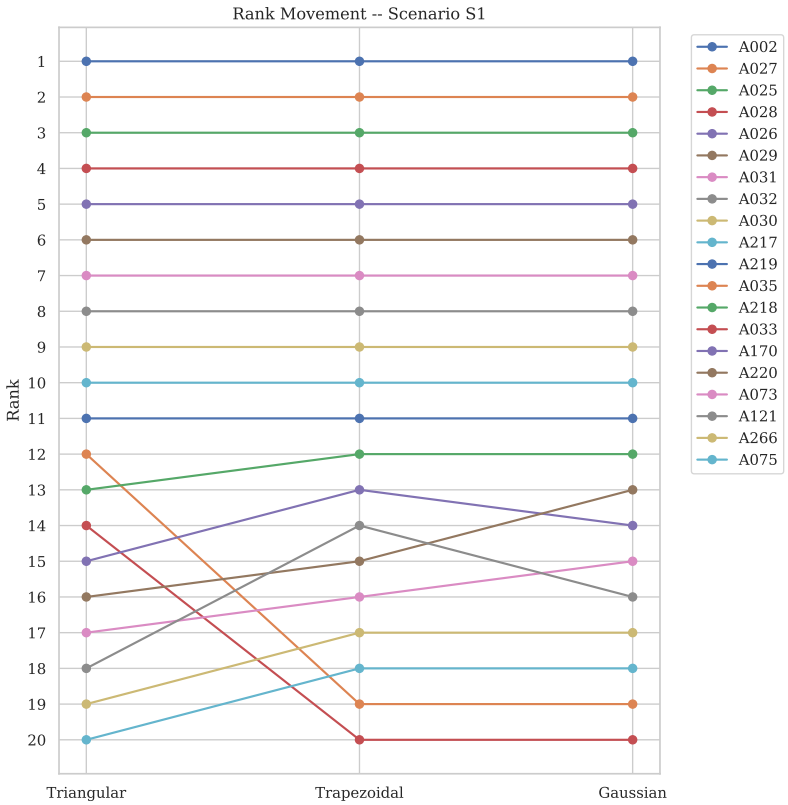


Figure 3.4: Rank-Position Movements in the Strong-Dominance Scenario

3.3.2. S2: All Alternatives Change Position

S2 exhibited the most extensive changes. All 20 alternatives moved by at least one position, and the mean displacement reached 4.20. A490 ranked first under the triangular and Gaussian functions but declined to fourth under the trapezoidal function. Conversely, A302 rose from eighth under the triangular function to second under the trapezoidal function before returning to eighth under the

Gaussian function. A473 exhibited the largest range of movement in S2, moving from rank 15 to rank 10 and then to rank 18.

This pattern cannot be explained solely by the contraction of the initial score range. The triangular and Gaussian functions remained reasonably aligned ($\rho = 0.8947$; $\tau_b = 0.8000$), whereas trapezoidal–Gaussian agreement declined to $\rho = 0.6752$ and $\tau_b = 0.4947$. In other words, S2 did not merely amplify random disturbance; it highlighted different responses across geometries.

Figure 3.5 shows crossings throughout the ranking range, in contrast to the concentration of changes in the lower positions under S1.

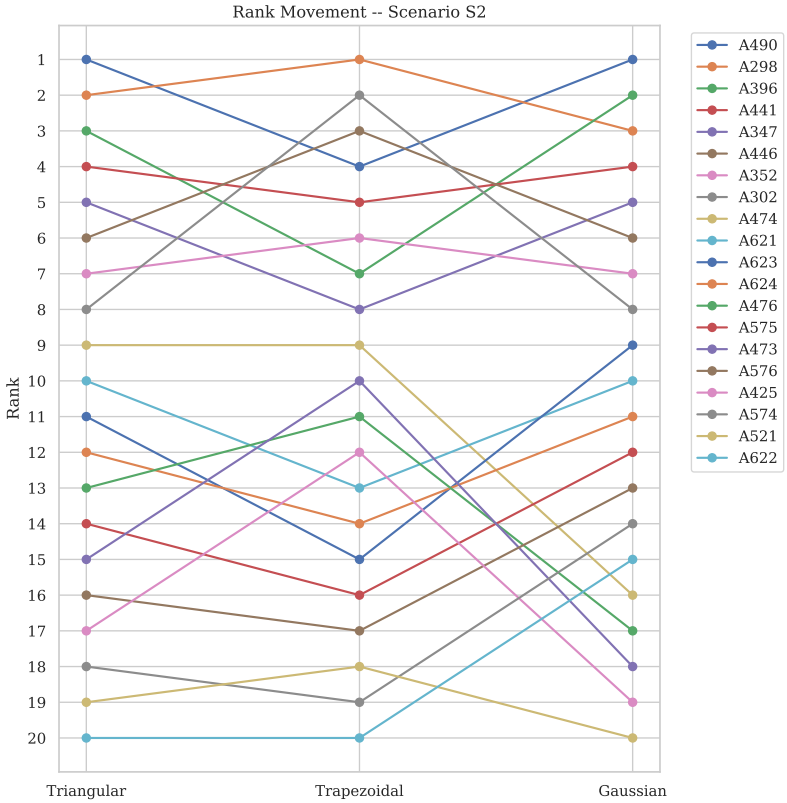


Figure 3.5: Rank-Position Movements in the Moderate-Competition Scenario

3.3.3. S3: Polarization between Graded Functions and the Plateau

S3 produced the sharpest findings. A101 remained first under all three functions, but nearly every other alternative changed position. The triangular and Gaussian functions produced almost identical orders, whereas the trapezoidal function generated a different structure. A398 moved from rank 7 under the triangular function to rank 2 under the trapezoidal function and rank 8 under the Gaussian function; A448 moved from 8 to 3 and then 7. The most extreme shifts were observed for A768 and A672. Both were ranked 9th and 10th, respectively, under the triangular and Gaussian functions, but fell to 19th and 20th under the trapezoidal function. Table 3.3 summarizes representative ranking changes across the three scenarios, highlighting the contrast between stable leading alternatives and substantial positional shifts induced by membership-function geometry.

Figure 3.6 shows that the triangular and Gaussian lines almost return to the same positions, whereas most crossings occur in the trapezoidal column. This visualization supports the interpretation that S3 instability is polarized: extreme closeness does not cause all functions to differ uniformly, but it magnifies the consequences of a function that levels micro-level differences.

Table 3.3: Representative Ranking Changes across Membership Functions

Scenario	Alternative	Case role	Tri.	Trap.	Gauss.
S1	A002	Stable top-ranked alternative	1	1	1
S1	A035	Most sensitive in S1	12	19	19
S2	A490	Changed leading candidate	1	4	1
S2	A302	Promotion under trapezoidal	8	2	8
S2	A473	Most sensitive in S2	15	10	18
S3	A101	Only unchanged position	1	1	1
S3	A398	Promotion under trapezoidal	7	2	8
S3	A448	Promotion under trapezoidal	8	3	7
S3	A768	Maximum decline	9	19	9
S3	A672	Maximum decline	10	20	10

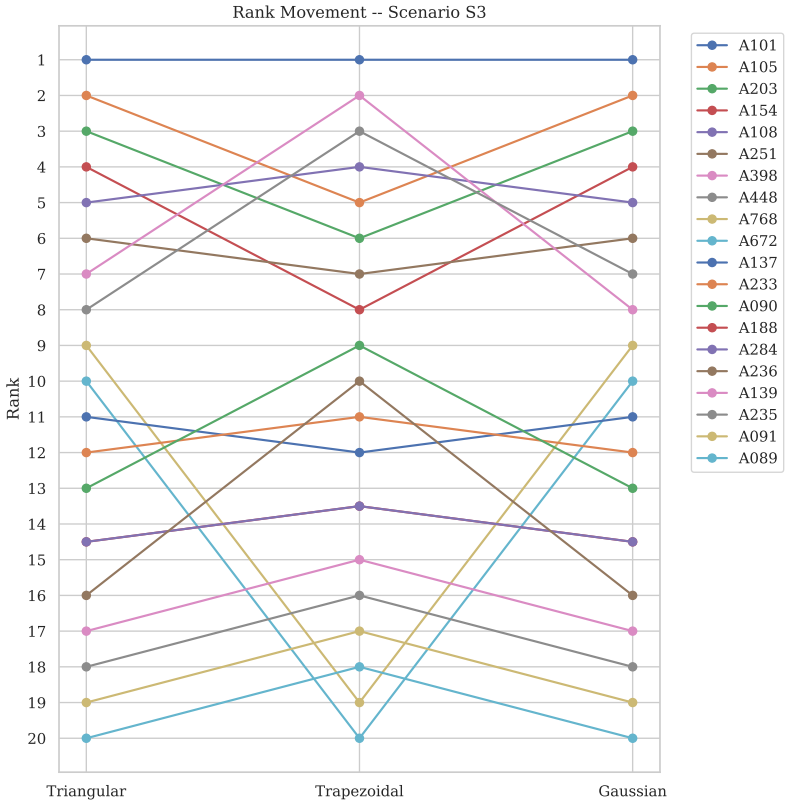


Figure 3.6: Rank-Position Movements in the Tight-Competition Scenario

3.4. Magnitude of Displacement and Ranking Agreement

The three displacement metrics in Table 3.4 capture different aspects of instability. The number of changed alternatives indicates the breadth of instability, mean displacement indicates typical severity, and maximum displacement identifies the risk of an extreme case. S2 was the scenario with the broadest instability and the highest mean displacement, whereas S3 produced the most extreme individual case.

Figure 3.7 underscores the difference in the breadth of instability: changes under S1 involved only nine alternatives, expanded to all alternatives under S2, and remained extensive under S3.

Table 3.4: Rank-Position Changes across Scenarios

Scenario	Mean displacement	Maximum displacement	Changed alternatives
S1	1.45	7	9 of 20
S2	4.20	8	20 of 20
S3	3.25	10	19 of 20

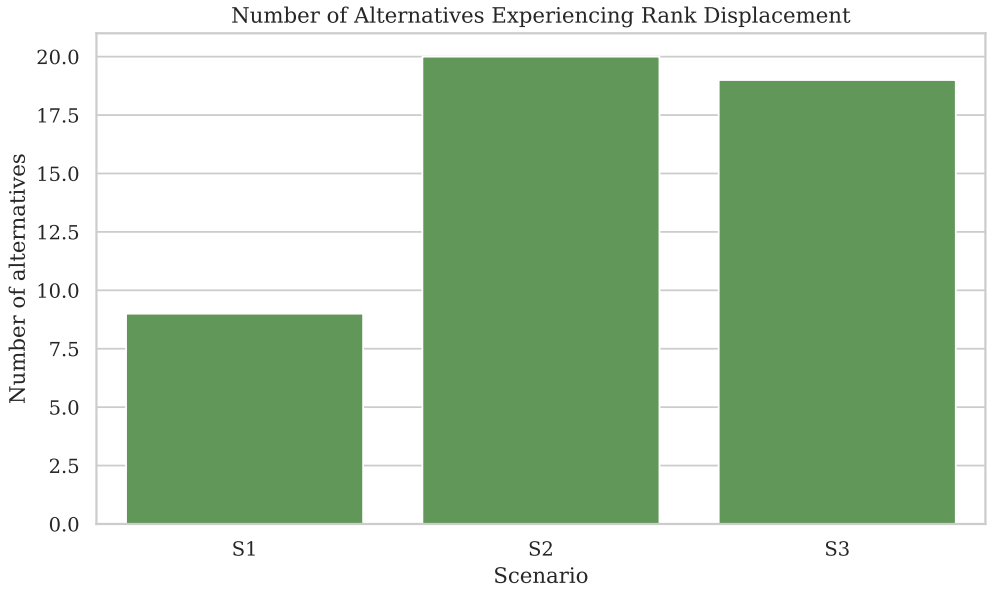


Figure 3.7: Number of Alternatives Experiencing Rank Displacement in Each Scenario

The correlation results in Table 3.5 complement the displacement metrics by measuring agreement in ranking structure. All pairs had $p < 0.05$, indicating that their ordinal association differed from zero at this sample size. These values do not demonstrate that two rankings are identical; stability must be interpreted from the magnitudes of ρ and τ_b, not from statistical significance alone.

Table 3.5: Ranking Correlations across Membership Functions

Scenario	Pair	ρ	p_ρ	τ_b	p_{τ_b}
S1	Triangular–Trapezoidal	0.9128	< 0.001	0.8421	< 0.001
	Triangular–Gaussian	0.9158	< 0.001	0.8526	< 0.001
	Trapezoidal–Gaussian	0.9925	< 0.001	0.9684	< 0.001
S2	Triangular–Trapezoidal	0.8707	< 0.001	0.6947	< 0.001
	Triangular–Gaussian	0.8947	< 0.001	0.8000	< 0.001
	Trapezoidal–Gaussian	0.6752	0.0011	0.4947	0.0018
S3	Triangular–Trapezoidal	0.7306	0.0003	0.5661	0.0005
	Triangular–Gaussian	0.9985	< 0.001	0.9894	< 0.001
	Trapezoidal–Gaussian	0.7291	0.0003	0.5556	0.0006

In S1, all pairs had $\rho > 0.91$ and $\tau_b > 0.84$. In S2, the largest decline occurred for the trapezoidal–Gaussian pair. In S3, the triangular–Gaussian pair recovered to almost perfect agreement, whereas

the two pairs involving the trapezoidal function remained at approximately $\rho = 0.73$ and $\tau_b = 0.56$. The mean coefficients by scenario summarize this pattern: S1 had $\bar{\rho} = 0.940$ and $\bar{\tau}_b = 0.888$, S2 declined to 0.814 and 0.663, whereas S3 increased slightly to 0.819 and 0.704 because of the nearly perfect triangular–Gaussian value. These averages must be read alongside the individual pairs; in S3, the aggregate values obscure substantial polarization. The only tied pair was A188–A284 in S3; both alternatives received average ranks under each membership function, and the reported coefficients therefore use the tie-aware definitions stated in the Methods section.

The patterns of the two measures are separately visualized in Figures 3.8 and 3.9. The Spearman heatmap emphasizes numerical positional proximity, whereas the Kendall heatmap displays a sharper decline because it is based on pairwise exchanges.

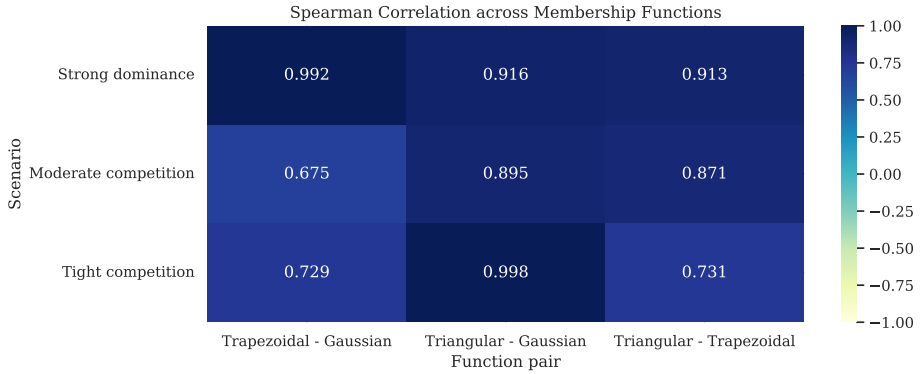


Figure 3.8: Spearman Correlations across Membership Functions in the Three Scenarios

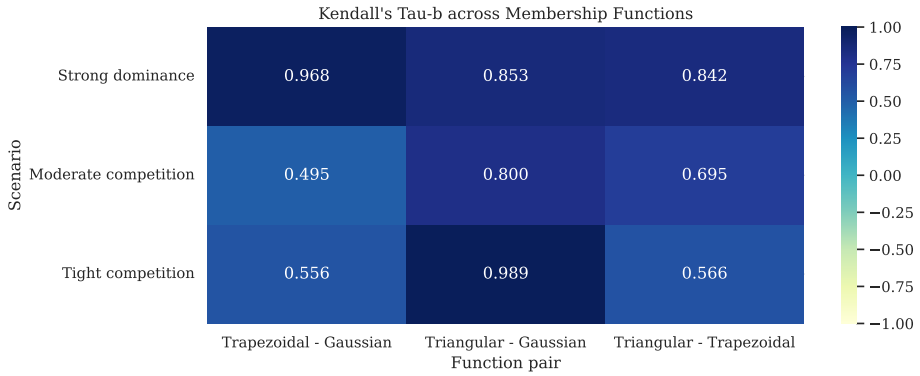


Figure 3.9: Kendall's Tau-b Correlations across Membership Functions in the Three Scenarios

Kendall's tau-b was consistently lower than Spearman's correlation in all nine comparisons. This result is consistent with the presence of numerous pairwise exchanges: Spearman summarizes the proximity of numerical positions, whereas Kendall directly counts the balance between concordant and discordant pairs while adjusting for ties. Consequently, using both measures provides a more complete picture than reporting only one ranking-similarity coefficient [29].

3.5. Interaction between Closeness and Function Geometry

The relationship between the competitive range and instability was not entirely monotonic. The reduction in $R(W_t)$ from 0.1051 in S1 to 0.0092 in S2 was followed by an increase in mean displacement from 1.45 to 4.20. When the range decreased further to 0.0020 in S3, mean displacement declined to 3.25, whereas maximum displacement increased to 10. Figure 3.10 illustrates this nonmonotonic

relationship: while the competitive range decreases consistently from S1 to S3, mean rank displacement reaches its maximum in S2. The lower mean in S3 occurred because the triangular and Gaussian functions again produced almost identical rankings, not because tight competition was safe.

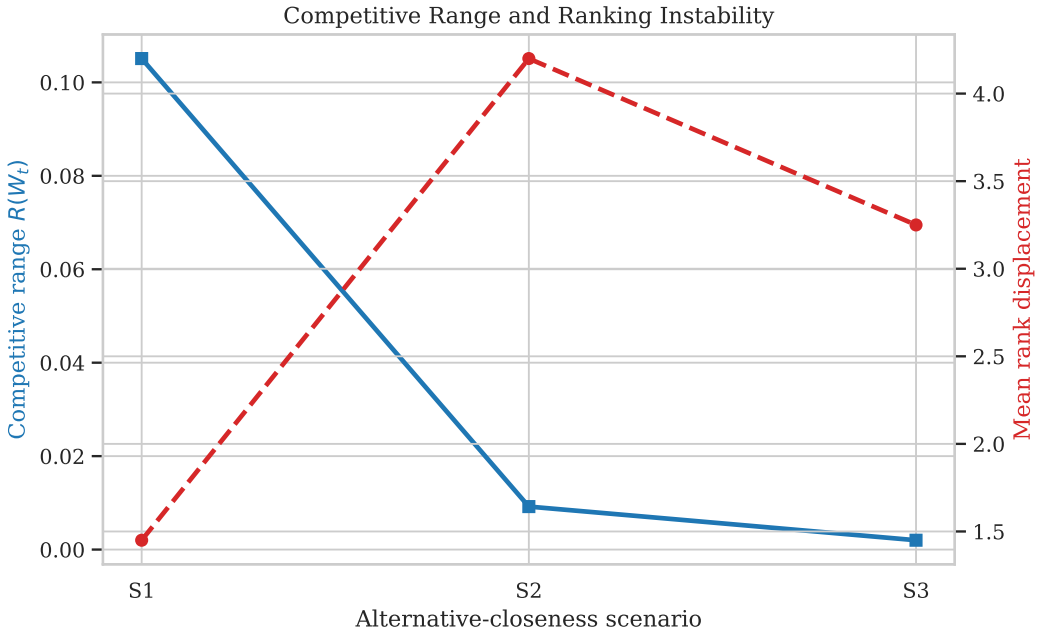


Figure 3.10: Competitive Range and Rank Displacement in Each Scenario

Figure 3.11 clarifies this interaction. Triangular–Gaussian agreement declined from S1 to S2 and then increased to $\tau_b = 0.9894$ in S3. By contrast, the two pairs involving the trapezoidal function degraded and remained near 0.56. Because the triangular function has a single peak and the Gaussian function retains a smooth gradient, micro-level differences continue to yield distinct outputs. A trapezoidal plateau can assign the same maximum membership degree to several nearby values, thereby removing part of the discriminative information before TOPSIS distances are calculated.

The plateau mechanism is consistent with the individual cases: in S3, A768 and A672 each fell by ten positions only under the trapezoidal function and returned to their original positions under the Gaussian function. However, these results do not support the claim that the trapezoidal function is always inferior. In S1, trapezoidal–Gaussian was in fact the most concordant pair ($\tau_b = 0.9684$). A more proportionate implication is that geometric effects are conditional on the locations of data relative to label centres and plateaus, as well as on score margins.

3.6. Discussion in Relation to the Literature and Contribution

The TOPSIS literature has shown that rankings can change when normalization, weights, alternative sets, or ideal points are modified [8, 11, 25–27]. This experiment identifies a related but distinct source of sensitivity: membership-function transformation can modify distance structure even when the dataset, weights, normalization, and TOPSIS procedure are held constant. The findings extend the discussion of ranking robustness from normalization and weighting stages to the fuzzy-representation stage.

The findings also relate to developments in Fuzzy TOPSIS that seek to preserve uncertainty and prevent information loss caused by premature transformation [15, 17]. In the present study, information loss was not measured through the width of fuzzy intervals but through its ordinal consequences. A trapezoidal plateau does not necessarily damage a ranking, but it may reduce discrimination when many values fall within the same core region. The contribution of this experiment is

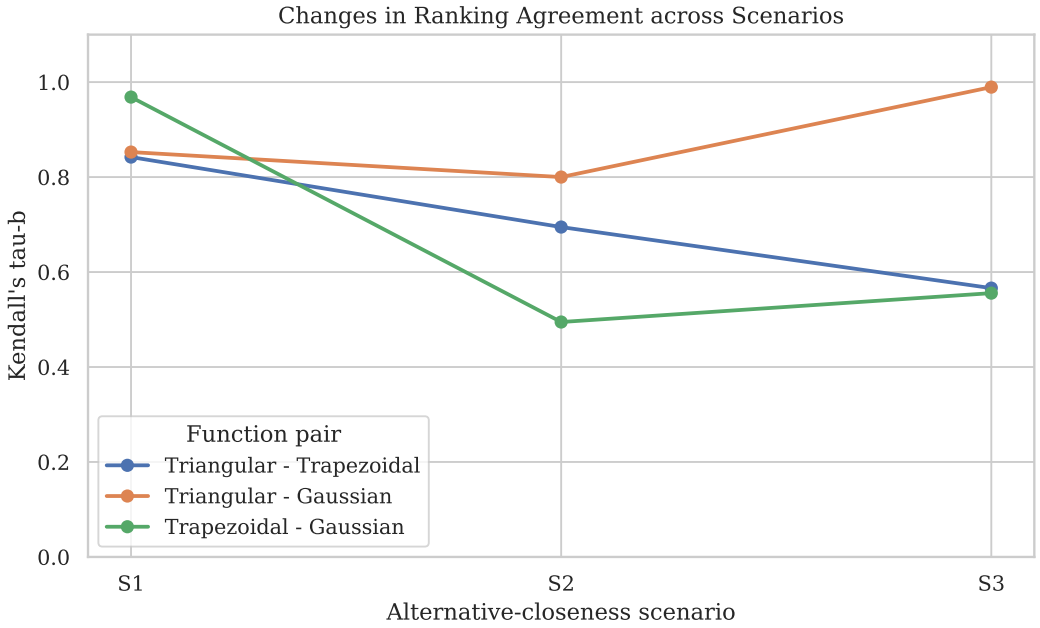


Figure 3.11: Changes in Kendall's Tau-b by Function Pair and Scenario

therefore not to identify a universally best function, but to show when the choice of geometry begins to constitute a decisive methodological decision.

The most important finding is the distinction between the *breadth* and *depth* of instability. S2 changed every alternative and had the largest mean displacement; S3 did not have the largest mean, but it produced the worst maximum displacement and the strongest function polarization. If only one metric were used, these two patterns would be conflated. A Fuzzy TOPSIS stability audit should therefore report, at minimum, the number of changed alternatives, mean and maximum displacement, and one position-based and one pairwise ranking-agreement measure.

3.7. Methodological Implications and Limitations

In practical applications, membership-function selection should not be based solely on ease of implementation. For candidates with closely matched scores, analysts should inspect the distribution of values relative to label centres and plateaus, run at least one comparison function, and report ranking stability alongside the final ranking. When important positions change across functions, the appropriate output is not to select one ranking arbitrarily, but to mark the decision as sensitive to model specification.

The generalizability of the findings is limited by the use of one dataset, three criteria, equal weights, a window size of 20, and one parameter configuration for each function. Equal weighting was deliberately used to isolate the two experimental factors, but ranking stability may differ under other weight structures. Only three points in the $R(W_t)$ distribution were tested; the experiment therefore does not estimate the form of a continuous relationship between alternative closeness and instability. The correlation p-values also do not test whether differences between coefficients are significant. Future research should sweep centre and width parameters, vary weights and window sizes, use multiple datasets, and examine other functions such as the *generalized bell*, sigmoidal, and type-2 functions. These limitations position the results as strong mechanistic evidence for the tested configuration rather than as a universal rule for all Fuzzy TOPSIS applications.

4. Conclusion

The experiment demonstrates that ranking stability in the tested membership-function-based Fuzzy TOPSIS variant is jointly determined by alternative closeness and membership-function geometry. Under strong dominance, all ranking pairs exhibited high correlations and the mean displacement was only 1.45 positions. As score margins narrowed, changing the membership function produced larger positional exchanges: all alternatives changed in the moderate-competition scenario, whereas the tight-competition scenario produced a maximum displacement of 10 positions.

Alternative closeness did not operate independently. In the tightest scenario, the triangular and Gaussian functions still produced almost identical rankings, with $\rho = 0.9985$ and $\tau_b = 0.9894$. The principal differences arose in pairs involving the trapezoidal function, for which $\tau_b \approx 0.56$. The plateau of this function rendered nearby values equivalent, causing part of the discriminative information to be lost before distances to the ideal solutions were calculated.

These findings support the use of alternative-closeness diagnostics and stability analyses when this membership-function-based Fuzzy TOPSIS variant is applied. When evaluating closely matched candidates, rankings obtained with a trapezoidal function should be compared with those obtained using triangular or Gaussian functions before they are used as a basis for decision-making. Further validation is required across different datasets, weights, window sizes, and membership-function parameters.

References

[1] H. Taherdoost and M. Madanchian, "Multi-criteria decision making (mcdm) methods and concepts," *Encyclopedia*, 2023. View online.

[2] Z. Wang, S. Nabavi, and G. P. Rangaiah, "Multi-criteria decision making in chemical and process engineering: Methods, progress, and potential," *Processes*, vol. 12, no. 11, 2024. View online.

[3] S. Chaube, S. Pant, A. Kumar, S. Uniyal, M. Singh, K. Kotecha, and A. Kumar, "An overview of multi-criteria decision analysis and the applications of ahp and topsis methods," *International Journal of Mathematical, Engineering and Management Sciences*, 2024. View online.

[4] M. Behzadian, S. K. Otaghsara, M. Yazdani, and J. Ignatius, "A state-of the-art survey of topsis applications," *Expert Systems with Applications*, vol. 39, pp. 13051–13069, 2012. View online.

[5] M. Madanchian and H. Taherdoost, "A comprehensive guide to the topsis method for multi-criteria decision making," *Sustainable Social Development*, 2023. View online.

[6] A. Aytekin, "Comparative analysis of the normalization techniques in the context of mcdm problems," *Decision Making: Applications in Management and Engineering*, 2021. View online.

[7] H. Dung, D. Trung, and V. Nguyen, "Comparison of multi-criteria decision making methods using the same data standardization method," *Strojnícky časopis - Journal of Mechanical Engineering*, vol. 72, pp. 57–72, 2022. View online.

[8] Z. Bánhidi and I. Dobos, "Sensitivity of topsis ranks to data normalization and objective weights on the example of digital development," *Central European Journal of Operations Research*, vol. 32, no. 1, pp. 29–44, 2024. View online.

[9] S. R. Nabavi, Z. Wang, and G. P. Rangaiah, "Sensitivity analysis of multi-criteria decision-making methods for engineering applications," *Industrial & Engineering Chemistry Research*, 2023. View online.

[10] N. T. D. Linh, N. H. Son, and D. X. Thao, "Evaluating the impact of weighting methods on the stability of scores for alternatives in multi-criteria decision-making problems," *Engineering, Technology & Applied Science Research*, vol. 15, no. 1, pp. 19998–20004, 2025. View online.

[11] E. Roszkowska, "Entropy and normalization in mcda: A data-driven perspective on ranking stability," *Entropy*, vol. 28, no. 1, p. 114, 2026. View online.

[12] C.-T. Chen, "Extensions of the topsis for group decision-making under fuzzy environment," *Fuzzy sets and systems*, vol. 114, no. 1, pp. 1–9, 2000. View online.

[13] A. Ishak and W. Wanli, "Analysis of fuzzy ahp-topsis methods in multi criteria decision making: Literature review," in *IOP Conference Series: Materials Science and Engineering*, vol. 1003, 2020. View online.

[14] N. Alkan and C. Kahraman, "Continuous intuitionistic fuzzy sets (cinfus) and their ahp&topsis extension: Research proposals evaluation for grant funding," *Applied Soft Computing*, vol. 145, p. 110579, 2023. View online.

[15] E. N. Madi, Z. A. Zakaria, A. Sambas, and Sukono, "Toward effective uncertainty management in decision-making models based on type-2 fuzzy topsis," *Mathematics*, vol. 11, no. 16, p. 3512, 2023. View online.

[16] M. C. Bozyigit and M. Ünver, "Parametric circular intuitionistic fuzzy information measures and multi-criteria decision making with extended topsis," *Granular Computing*, vol. 9, 2024. View online.

[17] A. Aminoroaya, A. Hadi-Vencheh, A. Jamshidi, and A. K. Yazdi, "Fuzzy topsis reinvented: Retaining linguistic information through interval-valued analysis," *Mathematics*, 2025. View online.

[18] S. H. Khairuddin, M. H. Hasan, M. Hashmani, and M. H. Azam, "Generating clustering-based interval fuzzy type-2 triangular and trapezoidal membership functions: A structured literature review," *Symmetry*, vol. 13, p. 239, 2021. View online.

[19] M. H. Azam, M. H. Hasan, S. Hassan, and S. Abdulkadir, "A novel approach to generate type-1 fuzzy triangular and trapezoidal membership functions to improve the classification accuracy," *Symmetry*, vol. 13, p. 1932, 2021. View online.

[20] A. Nieto-Morote and F. Ruz-Vila, "On the term set's semantics for pairwise comparisons in fuzzy linguistic preference models," *Entropy*, vol. 25, no. 5, p. 722, 2023. View online.

[21] A. K. Mallick, D. Ghosh, and K. Purkait, "A new approach to automatic and optimal membership function generation for fuzzy system modelling," *International Journal of Electrical and Electronics Engineering*, vol. 11, no. 8, 2024. View online.

[22] N. Ramli and N. Ahmad, "Expert elicitation of fuzzy membership functions of linguistic terms: A fire evacuation case study," *Journal of Information and Communication Technology*, vol. 24, no. 4, 2025. View online.

[23] R. Król, J. Więckowski, and J. Wątróbski, "Accuracy of the topsis method with different input data," *Procedia Computer Science*, vol. 207, pp. 4574–4583, 2022. View online.

[24] S. A. Sadabadi, A. Hadi-Vencheh, A. Jamshidi, and M. Jalali, "An improved fuzzy topsis method with a new ranking index," *International Journal of Information Technology & Decision Making*, vol. 21, no. 02, pp. 615–641, 2022. View online.

[25] S. Mousavi-Nasab and A. Sotoudeh-Anvari, "A new multi-criteria decision making approach for sustainable material selection problem: A critical study on rank reversal problem," *Journal of Cleaner Production*, vol. 182, pp. 466–484, 2018. View online.

[26] B. Yang, J. Zhao, and H. Zhao, "A robust method for avoiding rank reversal in the topsis," *Computers & Industrial Engineering*, vol. 174, p. 108776, 2022. View online.

[27] L. Jiang, H. Liao, and B. De Baets, "A simulation study on the probabilities of rank reversal, tie making, and tie breaking for multiple criteria decision making methods," *Omega*, vol. 125, p. 103033, 2024. View online.

[28] P. Karande, E. K. Zavadskas, and S. Chakraborty, "A study on the ranking performance of some mcdm methods for industrial robot selection problems," *International Journal of Industrial Engineering Computations*, vol. 7, no. 3, pp. 399–422, 2016. View online.

[29] W. Sałabun and K. Urbaniak, "A new coefficient of rankings similarity in decision-making problems," in *International Conference on Computational Science*, pp. 632–645, Springer, 2020. View online.
[30] A. Tsanas and A. Xifara, "Energy efficiency," 2012. View online.

IEEE Citation Format:
M. N. Jauhari *et al.*, *"Fuzzy TOPSIS Ranking Stability under Membership-Function Variations across Alternative-Closeness Scenarios"*, *Jurnal Diferensial*, vol. 8(2), pp. 201-218, 2026.

This work is licensed under a Creative Commons "Attribution-ShareAlike 4.0 International" license.

